$AVPO_4F$ (A = Li, K) : A 4 V cathode material for high-power rechargeable batteries

$AVPO_4F$ (A = Li, K): a new 4V cathode material for high-power rechargeable batteries

Stanislav S. Fedotov*[,†,‡], Nellie R. Khasanova[†], Aleksandr Sh. Samarin[†], Oleg A. Drozhzhin[†], Dmitry Batuk[§], Olesia M. Karakulina[§], Joke Hadermann[§], Artem M. Abakumov[†,‡,§] and Evgeny V. Antipov[†]

[†]Department of Chemistry, Lomonosov Moscow State University, 119991 Moscow, Russian Federation

[‡]Skoltech Center for Electrochemical Energy Storage, Skolkovo Institute of Science and Technology, 143026 Moscow, Russian Federation

[§]EMAT, University of Antwerp, Groenenborgerlaan 171, B-2020, Antwerp, Belgium

ABSTRACT: A novel potassium-based fluoride-phosphate, $KVPO_4F$, adopting the $KTiOPO_4$ (KTP) type structure is synthesized and characterized. About 85% of potassium has been electrochemically extracted on oxidation producing a cathode material with attractive performance for Li-ion batteries. The material operates at an electrode potential near 4 V vs Li/Li^+ exhibiting a sloping voltage profile, extremely low polarization, a small volume change of about 2% and excellent rate capability, maintaining more than 75% of the initial capacity at 40 C discharge rate without significant fading.

Recently fluoride-phosphate based cathode materials for Li-ion batteries have captured much attention because they can combine the benefits of both anionic species and demonstrate higher structural diversity. In fact, the incorporation of fluorine brought about several advantages compared to oxide materials, namely, the increase in the operating voltage due to a higher electronegativity and better kinetics arising from a lower affinity of lithium to the fluoride anion. The first fluoride-phosphate cathode, $LiVPO_4F$, with the tavorite structure was introduced by Barker et al.[1] It exhibited an 0.4 V higher redox potential (4.2 V vs Li/Li^+) than fluorine-free Nasicon-type $Li_3V_2(PO_4)_3$ (3.8 V vs Li/Li^+)[2] as well as a substantial specific capacity of 156 mAh/g. This finding boosted the examination of different families of fluoride-containing materials such as fluoride-phosphates A_2MPO_4F (A = Li, Na; M = Mn, Fe, Co, Ni)[3-9] and fluoride-sulfates $LiMSO_4F$ (M = Mn, Fe, Zn)[11-14], which are also famous for their rich polymorphism. In these systems the crystal structure strongly affects the key electrochemical properties[14,15]. For instance, $LiFeSO_4F$ with triplite structure displays an operating potential 0.3 V higher than tavorite[10,11,13], the potential of Li_2FePO_4F varies depending on the crystalline form, i.e. 2.9 V in tavorite-type[7], 3.3 V in layered[8] and 3.4 V in stacked[9]. Generally, the direct synthesis of some Li-containing polymorphs is difficult due to thermodynamic reasons. In such cases sodium-containing counterparts with a desirable framework motif are commonly used with a subsequent chemical or electrochemical exchange of Na by Li leading to target cathode materials[8,9,16]. In this sense K provides even ampler opportunities than Na for searching and stabilizing new structures due to a larger ionic radius and somewhat different crystal chemistry. With this idea in mind Tarascon's group proposed $KFeSO_4F$ cathode[17] with $KTiOPO_4$ (KTP) structure anticipating unique electrochemical properties. Indeed, the extraction of potassium ions resulted in a steady $FeSO_4F$ framework suitable for reversible de/intercalation of Li, Na and even K ions.

Motivated by this work we endeavored to design phosphate-containing KTP-like compounds with higher energy density and stability. For this purpose we screened existing KTP structures and found potassium vanadyl phosphate $KVOPO_4$ that satisfies the higher specific energy requirement[18]. However, a full conversion of V^{4+} to V^{5+} in an electrochemical cell might cause serious structural distortions induced by changing vanadium coordination from an octahedron (V^{+4}) to a square-pyramid characteristic to V^{+5}. This will inevitably introduce strain accelerating the electrode degeneration. To address these issues, we propose a replacement of V^{4+} by V^{3+} with a simultaneous substitution of O^{2-} by F^- to preserve the electroneutrality which results in a $KVPO_4F$ formula. It should be noted that KTP-type $KMPO_4F$ (M= Al, Cr, Fe)[19-21] counterparts are known however they have never been considered as electrode materials for rechargeable batteries. Here we report on a novel vanadium-based cathode material $AVPO_4F$ (A = Li, K) adopting a KTP-type framework for high power rechargeable batteries with enhanced specific energy and excellent rate capability. To the best of our knowledge, this is the first compound with a KTP structure containing both vanadium and fluorine.

$KVPO_4F$ was synthesized via freeze-drying assisted solid-state route in two steps. First, vanadium phosphate VPO_4 was obtained. For this NH_4VO_3 (99.9%) and $NH_4H_2PO_4$ (99.99%) were dissolved in distilled H_2O under stirring at 70°C with a drop-wise addition of an ascorbic acid solution as a carbon source and reducing agent. The resulting clear blue-colored solution was dispersed into liquid nitrogen and sublimated at low pressure (10^{-2} bar) within 72 hours. The obtained cryogranulated powder was annealed at 800°C for 7 hours. The residual carbon content in VPO_4 was estimated by thermogravimetric analysis to be ~3 wt. %. Then the product was mixed with the equimolar amount of KHF_2 (99.9%), grinded and fired in an Ar flow at 600°C for 1h followed by quenching to room temperature.

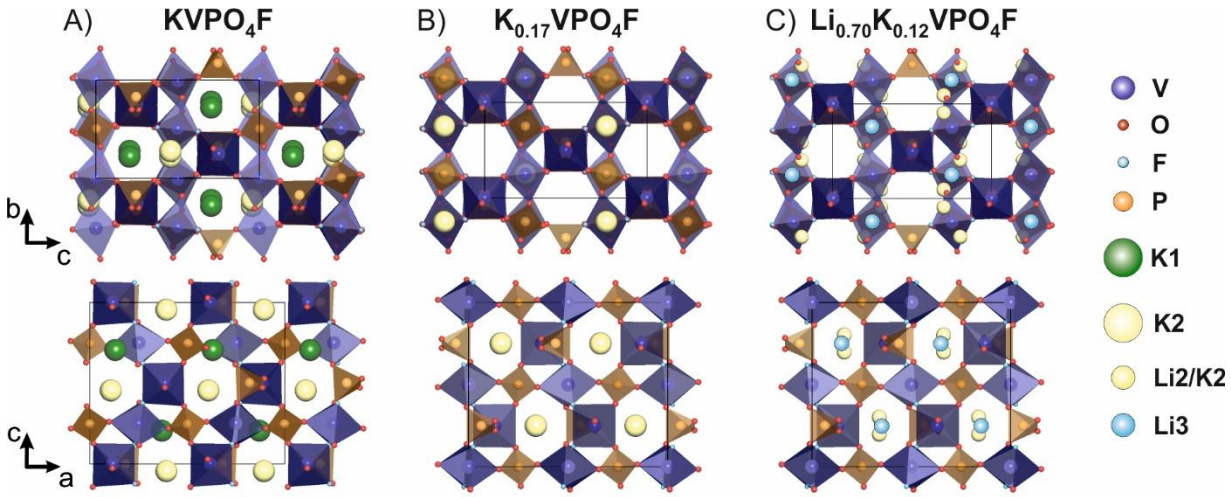

Figure 1. Crystal structures of $KVPO_4F$, $K_{0.17}VPO_4F$, $Li_{0.70}K_{0.12}VPO_4F$ shown along [100] and [010] directions.

According to the powder XRD analysis, this synthetic procedure resulted in a phase-pure $KVPO_4F$ sample. The material consists of elongated rounded particles of 200–400 nm in the long direction determined by SEM (figure S1 of Supporting information (SI)). The bulk K : V : P ratio measured by ICP-AES, 0.31(2):0.34(2):0.35(2), is consistent with TEM-EDX data, 0.33(1):0.32(1):0.35(2), acquired on individual particles. Also, TEM-EDX undeniably demonstrates the presence of fluorine in $KVPO_4F$ (fig. S2 of SI). To analyze a possible F^-/OH^- mixing in $KVPO_4F$, FT-IR spectroscopy analysis was performed. No characteristic bands in the 1500–4000 cm^{-1} region were identified (fig. S3 of SI), which clearly confirms the absence of either –OH or adsorbed water.

The structure of $KVPO_4F$ was refined from powder XRD data (fig. S4 of SI) using the Rietveld method with JANA2006 program[22]. The $KFeSO_4F$ structure was used as a starting model[17]. The powder diffraction pattern was fully indexed on an orthorhombic lattice (S.G. #33 $Pna2_1$) with $a = 12.8200(3)$ Å, $b = 6.3952(1)$ Å, $c = 10.6115(2)$ Å. No additional ordering or superstructure was detected with electron diffraction (fig. S5 of SI). The main crystallographic parameters, atomic positions, atomic displacement parameters and main interatomic distances are given in tables S1-3 of SI. The refined structure was confirmed using aberration-corrected high angle annular dark field scanning transmission electron microscopy (HAADF-STEM) images taken along the [100] and [010] directions (fig. S6 of SI).

$KVPO_4F$ is built up of helical chains of the VO_4F_2 octahedra and PO_4 tetrahedra forming a rigid framework hosting potassium ions in a 3D system of continuous spatial cavities (fig. 1A). Alternating VO_4F_2 octahedra are corner-shared through fluorine atoms located in two equatorial (*cis*) positions for V1 and two axial (*trans*) positions for V2, with other four oxygen corners being shared with PO_4 tetrahedra. The average V–X (X = O, F) interatomic distances for both metal sites are 1.98 Å characteristic to a V^{3+} environment. The bond valence sum for V1 and V2 is 3.15(6) validating +3 oxidation state of vanadium. The other confirmation comes from the EELS spectrum (fig. S7 of SI) showing the V $L_{2,3}$ edge typical for V^{3+} in the octahedral coordination. Potassium in the structure occupies two 9-coordinated positions, K1 and K2, located in the open tunnels along the *a* and *b* axes respectively (fig. 1A).

For the electrochemical evaluation the initial $KVPO_4F$ material was oxidized by charging up to 4.8 V vs Li/Li^+ at C/20 rate and holding at this potential for 5 hours (fig. S8 of SI). The charged electrode was recovered, washed twice with dimethyl carbonate (DMC) and put into a fresh cell with a new portion of electrolyte and Li-foil anode for further testing. According to the EDX data, potassium in not completely removed and about 15% remains in the structure. Therefore we ascribe the $K_{0.15}VPO_4F$ composition to the oxidized material. Such a possibility to produce vanadium phosphate frameworks by electrochemical oxidation was first shown by Song[23] et al, who formed a new ε-$VOPO_4$ polymorph from a H_2VOPO_4 precursor.

The obtained $K_{0.15}VPO_4F$ material was cycled in a galvanostatic regime within the 2.0–4.7 V vs Li/Li^+ potential range at different rates from C/5 to 40C showing an uptake of 0.7 Li per formula unit at the average voltage of ~4 V. $K_{0.15}VPO_4F$ exhibits a sloping voltage profile indicating of a solid-solution-like de/intercalation mechanism which is favorable to high power applications (fig. 2).

To get insight into structural and compositional changes taking place in the electrochemical cell an *ex situ* investigation was performed on recovered electrode materials. The detailed information on the preparation of the oxidized and lithiated electrode materials is given in SI section. The XRD patterns of the recovered electrodes displayed a close resemblance with those of the initial material confirming the KTP–type structure is preserved (fig. S9 of SI). Because of insufficient quality of *ex-situ* XRD patterns, selected area electron diffraction (SAED) and electron diffraction tomography (EDT) were applied to examine the crystal structure of the recovered electrode materials. The electron diffraction study revealed that in contrast to the noncentrosymmetric parent $KVPO_4F$ phase ($Pna2_1$) the crystal structures of both oxidized and lithiated electrode materials possess a centrosymmetric space group (*Pnan*) (fig. S10 of SI). The cell parameters refined from *ex-situ* XRD with the determined space group were taken for the refinement of atomic positions and occupancies using EDT data. All details of the refinement are described in the SI.

The structure refinement of the oxidized electrode indicated the K1 site is empty and all residual K is located in the K2 position in the voids along the [010] direction (fig. 1B). The refined amount of residual K (~17%) gave the $K_{0.17}VPO_4F$ formula consistent with the bulk EDX measurements (~15%). A complete removal of K is likely

to occur at potentials over 5 V that may be accompanied by a severe electrolyte decomposition or degradation of the material itself. At the same time, the residual K in the oxidized material might stabilize the "VPO_4F" framework by "pillaring" the tunnels.

The crystal structure refinement of the discharged material revealed that the intercalation of lithium takes place in the channels along [010] leaving the channels along [100] unoccupied. The inserted Li shares the K2 site with the residual potassium and creates a new Li3 position, which was localized using a difference Fourier map (fig S12 of SI). The refined occupancy for K turned out to be 0.12 and the amount of the inserted Li^+ ions was calculated from the electrochemical measurements as 0.7. The latter was taken as a constraint during the refinement which resulted in the $Li_{0.70}K_{0.12}VPO_4F$ composition. The Li3 has a [4+2] coordination with four short 1.99–2.14 Å Li3–O bonds. It resides in the channels along the *b* axis forming an alternating row with Li2 atoms (fig. 1C). The main crystallographic parameters, structure information and interatomic distances of the oxidized and lithiated materials are given in tables S4–8.

According to the structure refinement, the electrochemically cycled material preserves the KTP framework, but the accommodation of Li does not completely follow the initial crystallographic positions of K. The difference in the unit cell volume of all three phases is small and does not exceed 2.2% (table S1, S4 of SI) in contrast to tavorite-type $LiVPO_4F$ which exhibits an 8.5% volume change between charged and discharged forms[24]. The slight decrease of the cell parameters of the lithiated material can be explained in terms of Coulomb interactions between the oxygen framework and the new Li3 ions inserted in the channels along the *b*-axis. It reduces the *a* and *c* parameters while the *b* parameter remains almost the same.

To analyze diffusion paths in the crystal structure, the bond valence sum mapping (BVSM)[25] method was utilized. In the initial $KVPO_4F$ structure K^+ ions follow a curved pathway along the *c* axis (fig. S14a of SI). This is in good agreement with ionic conductivity measurements the isostructural KTP materials, which revealed the highest conductivity values along the *c*-direction (10^{-4}–10^{-6} S/cm along *c* vs 10^{-7}–10^{-10} S/cm along *a* and *b*, 400 K)[26,27]. In the oxidized material the Li^+ diffusion map becomes three-dimensional (fig. S14b of SI). In this case, we cannot observe a distinct "pathway" for the Li^+ ions because of their tiny radius compared to the radius of the channels. The obtained stretched diffusion map implies a high mobility for the Li^+ ions that was confirmed by the electrochemical testing.

$Li_xK_{0.15}VPO_4F$ shows remarkable capacity retention at 40C maintaining more than 50% of theoretical (156 mAh/g) or 75% of initial specific capacity (111 mAh/g at C/5) (fig. 3). Extended cycling was carried out at a rate of 1C. After 100 cycles a moderate capacity fading of 27% with a Coulomb efficiency over 99% was observed (insert in fig. 2).

An extremely low polarization observed (fig. S13 of SI) is likely due comparably high ionic and electronic conductivities of this material. Apparently, Li ion diffusion in $Li_xK_{0.15}VPO_4F$ is not hindered by "pinning" interactions with the lattice as it occurs in case of $FeSO_4F$[19]. Presumably, it is due to the smaller but much more suitable channels in the "VPO_4F" framework (ionic radius of V^{+3}, 0.64 Å comparing to that of Fe^{2+}, 0.78 Å). Rapid kinetics of the Li de/intercalation is also evidenced by rate capability measurements (fig. 3).

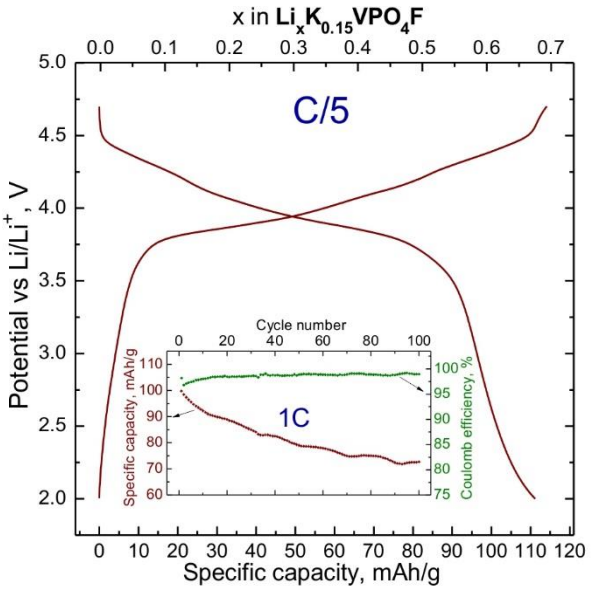

Figure 2. A typical charge-discharge curve of $Li_xK_{0.15}VPO_4F$ at C/5. The inset demonstrates the capacity retention and Coulomb efficiency in the cycling ability test at 1C rate.

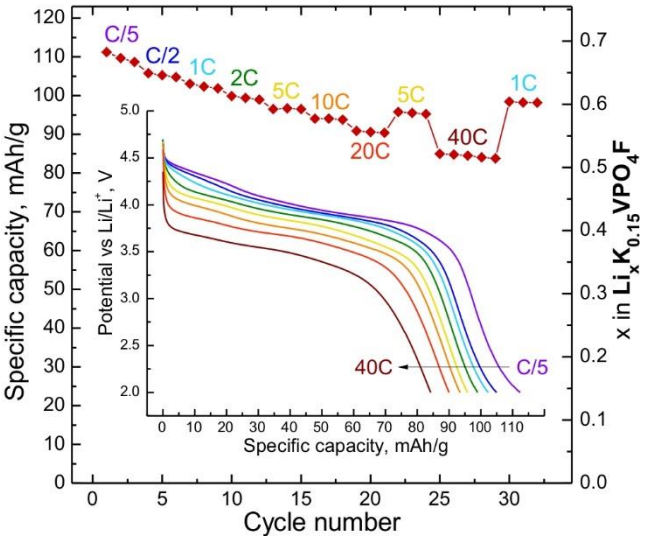

Figure 3. C-rates capability upon cycling and corresponding discharge curves of $Li_xK_{0.15}VPO_4F$. Before each discharge, the cells were charged up to 4.7 V at C/5 for the first three cycles and then at C/2 rate starting from the 4th cycle.

It should be noted that this material also exhibits reversible capacity at potentials around 2 V (fig. S15 of SI) indicating a multi-redox process similar to $LiVPO_4F$ tavorite[1,24]. This electrochemical activity in a low-voltage domain needs further investigation.

The obtained cathode material reveals remarkable electrochemical properties in a Li-anode cell. After optimization it can compete with many renowned materials in terms of energy density or rate capability. The theoretical 624 Wh/kg specific energy of $Li_xK_{0.15}VPO_4F$ exceeds that of $LiFePO_4$ (583 Wh/kg) and is comparable to that of tavorite $LiVPO_4F$ (655 Wh/kg). A significant advantage of the discovered material is its much smaller volume variation upon cycling in comparison with the latter ones.

The possibility to operate at 40C preserving a substantial capacity level and retention makes it a serious contender to existing high-

power cathodes such as NASICON-type $Li_3V_2(PO_4)_3$. Due to the presence of spatial voids and channels $Li_xK_{0.15}VPO_4F$ obviously has a slightly lower volumetric energy density (~2000 Wh/l) compared to $LiFePO_4$ (2135 Wh/l) or tavorite-$LiVPO_4F$ (2140 Wh/l) which is still attractive for high-power or large-scale applications.

ASSOCIATED CONTENT

Supporting Information. Experimental details, SEM and TEM images, typical EDX spectrum for $KVPO_4F$, ED patterns for $KVPO_4F$, $K_{0.15}VPO_4F$ and $Li_{0.70}K_{0.12}VPO_4F$, FTIR and EELS spectra, results of Rietveld refinement of KVPO4F, details of structure solution for $K_{0.15}VPO_4F$ and $Li_{0.70}K_{0.12}VPO_4F$ using EDT, crystallographic parameters for the refine structures, BVS maps, electrochemical data. These materials are available free of charge via the Internet at http://pubs.acs.org.

AUTHOR INFORMATION

Corresponding Author

* E-mail: fedotov.msu@gmail.com

Author Contributions

The manuscript was written through contributions of all authors.

Notes

Authors declare no competing financial interests

ACKNOWLEDGMENT

The authors kindly thank Dr. S. N. Putilin for XRD measurements, Dr. O. A. Shlyakhtin for the assistance in freeze-drying synthesis, Dr. A. V. Mironov for fruitful discussions, A. A. Sadovnikov for SEM imaging and E. A. Karpukhina for FTIR spectra. The work was partly supported by Russian Science Foundation (grant 16-19-00190), Skoltech Center for Electrochemical Energy Storage and Moscow State University Development Program up to 2020. J. Hadermann, O. M. Karakulina and A. M. Abakumov acknowledge support from FWO under grant G040116N.

REFERENCES

(1) Barker, J.; Saidi, M. Y.; Swoyer, J. L. Electrochemical Insertion Properties of the Novel Lithium Vanadium Fluorophosphate, $LiVPO_4F$. *J. Electrochem. Soc.* **2003**, *150*, A1394–A1398.

(2) Gaubicher, J.; Wurm, C.; Goward, G.; Masquelier, C.; Nazar, L. F. Rhombohedral Form of $Li_3V_2(PO_4)_3$ as a Cathode in Li-Ion Batteries. *Chem. Mater.* **2000**, *12*, 3240–3242.

(3) Dutreilh, M.; Chevalier, C.; El-Ghozzi, M.; Avignant, D.; Montel, J. M. Synthesis and Crystal Structure of a New Lithium Nickel Fluorophosphate $Li_2[NiF(PO_4)]$ with an Ordered Mixed Anionic Framework. *J. Solid State Chem.* **1999**, *142*, 1–5.

(4) Okada, S.; Ueno, M.; Uebou, Y.; Yamaki, J. Fluoride Phosphate Li_2CoPO_4F as a High-Voltage Cathode in Li-Ion Batteries. *J. Power Sources* **2005**, *146*, 565–569.

(5) Khasanova, N. R.; Gavrilov, A. N.; Antipov, E. V.; Bramnik, K. G.; Hibst, H. Structural Transformation of Li_2CoPO_4F upon Li-Deintercalation. *J. Power Sources* **2011**, *196*, 355–360.

(6) Kim, S.-W.; Seo, D.-H.; Kim, H.; Park, K.-Y.; Kang, K. A. Comparative Study on Na_2MnPO_4F and Li_2MnPO_4F for Rechargeable Battery Cathodes. *Phys. Chem. Chem. Phys.* **2012**, *14*, 3299–3303.

(7) Ramesh, T. N.; Lee, K. T.; Ellis, B. L.; Nazar, L. F. Tavorite Lithium Iron Fluorophosphate Cathode Materials: Phase Transition Electrochemistry of $LiFePO_4F$–Li_2FePO_4F. *Electrochem. Solid-State Lett.* **2010**, *13*, A43–A47.

(8) Ellis, B. L.; Makahonouk, W. R. M.; Makimura, Y.; Toghill, K.; Nazar, L. F. A Multifunctional 3.5 V Iron-Based Phosphate Cathode for Rechargeable Batteries. *Nat. Mater.* **2011**, *10*, 772–779.

(9) Khasanova, N. R.; Drozhzhin, O. A.; Storozhilova, D. A.; Delmas, C.; Antipov, E. V. New Form of Li_2FePO_4F as Cathode Material for Li-Ion Batteries. *Chem. Mater.* **2012**, *24*, 4271–4273.

(10) Recham, N.; Chotard, J.-N.; Dupont, L.; Delacourt, C.; Walker, W.; Armand, M.; Tarascon, J.-M. A 3.6 V Lithium-Based Fluorosulphate Insertion Positive Electrode for Lithium-Ion Batteries. *Nat. Mater.* **2010**, *9*, 68–74.

(11) Barpanda, P.; Ati, M.; Melot, B. C.; Rousse, G.; Chotard, J.-N.; Doublet, M.-L.; Sougrati, M. T.; Corr, S. A.; Jumas, J.-C.; Tarascon, J. M. A 3.90 V Iron-Based Fluorosulphate Material for Lithium-Ion Batteries Crystallizing in the Triplite Structure. *Nat. Mater.* **2011**, *10*, 772–779.

(12) Ati, M.; Melot, B. C.; Rousse, G.; Chotard, J.-N.; Barpanda, P.; Tarascon, J. M. Structural and Electrochemical Diversity in $LiFe_{1-\delta}Zn_\delta SO_4F$ Solid Solution: A Fe-Based 3.9 V Positive-Electrode Material. *Angew. Chem. Int. Ed.* **2011**, *50*, 10574–10577.

(13) Ben Yahia, M.; Lemoigno, F.; Rousse G.; Boucher, F.; Tarascon J.-M.; Doublet, M.-L. Origin of the 3.6 V to 3.9 V Voltage Increase in the $LiFeSO_4F$ Cathodes for Li-Ion Batteries. *Energy Environ. Sci.* **2012**, *5*, 9584–9594.

(14) Antipov, E. V.; Khasanova, N. R.; Fedotov, S. S. Perspectives on Li and Transition Metal Fluoride Phosphates as Cathode Materials for a New Generation of Li-Ion Batteries. *IUCrJ* **2015**, *2*, 85–94.

(15) Melot, B. C.; Scanlon, D. O.; Reynaud, M.; Rousse, G.; Chotard, J.-N.; Henry, M.; Tarascon, J.-M. Chemical and Structural Indicators for Large Redox Potentials in Fe-Based Positive Electrode Materials. *ACS Appl. Mater. Interfaces* **2014**, *6*, 10832–10839.

(16) Shirane, T.; Kanno, R.; Kawamoto, Y.; Takeda, Y.; Takano, M.; Kamiyama, T.; Izumi, F. Structure and Physical Properties of Lithium Iron Oxide, $LiFeO_2$, Synthesized by Ionic Exchange Reaction. *Solid State Ionics* **1995**, *79*, 227–233.

(17) Recham, N.; Gwenaelle, R.; Sougrati, M. T.; Chotard, J.-N.; Frayret, C.; Mariyappan, S.; Melot, B. C.; Jumas, J.-C.; Tarascon, J.-M. Preparation and Characterization of a Stable $FeSO_4F$-Based Framework for Alkali Ion Insertion Electrodes. *Chem. Mater.* **2012**, *24*, 4363–4370.

(18) Phillips, M. L. F.; Harrison, W. T. A.; Gier, T. E.; Stucky, G. D.; Kulkarni, G. V.; Burdett, J. K. Electronic Effects of Substitution Chemistry in the Potassium Titanyl Phosphate ($KTiOPO_4$) Structure Field: Structure and Optical Properties of Potassium Vanadyl Phosphate. *Inorg. Chem.* **1990**, *29*, 2158–2163.

(19) Slovokhotova, O. L.; Ilyushin, G. D.; Triodina, N. S.; Mel'nikov, O. K.; Dem'yanets, L. N.; Gerr, R. G.; Tsirel'son, V. G. Features of the Atomic and Electronic Structure of the New Nonlinear Optical Crystal $KAlFPO_4$. *Zhurnal Strukturnoi Khimii* **1991**, *32*, 103–109.

(20) Slobodnyak, N. S.; Nagorniy, P. G.; Kornienko, Z. I.; Kapshuk A. A. Crystal Structure of $KCrFPO_4$ (in Russian). *Zhurnal Neorganicheskoi Khimii* **1991**, *36*, 1390–1392

(21) Belokoneva, E. L.; Yakubovich, O. V.; Tsirel'son, V. G.; Urusov, V. S. Crystal and Electron Structure of the Nonlinear Crystal $KFeFPO_4$ - a Structural Analog of $KTiOPO_4$. *Izvestiya Akademii Nauk SSSR, Neorganicheskie Materialy*, **1990**, *26*, 595–601

(22) Petricek, V., Dusek, M.; Palatinus, L. Crystallographic Computing System JANA2006: General Features. *Z. Kristallogr.* **2014**, *229*, 345–352.

(23) Song, Y.; Zavalij, P. Y.; Whittingham, M. S., ε-$VOPO_4$: Electrochemical Synthesis and Enhanced Cathode Behavior. *J. Electrochem. Soc.* **2005**, *152*, A721–A728.

(24) Ellis, B. L.; Ramesh, T. N.; Davis, L. J. M.; Goward, G. R.; Nazar, L. F. Structure and Electrochemistry of Two-Electron Redox Couples in Lithium Metal Fluorophosphates Based on the Tavorite Structure. *Chem. Mater.* **2011**, *23*, 5138–5148

(25) Sale, M.; Avdeev, M. 3DBVSMAPPER: a Program for Automatically Generating Bond-Valence Sum Landscapes. *J. Appl. Cryst.* **2012**, *45*, 1054–1056.

(26) Furusawa, Sh-I; Hayasi, H.; Ishibashi, Y.; Miyamoto, A.; Sasaki, T. Ionic Conductivity of Quasi-One-Dimensional Superionic Conductor $KTiOPO_4$ (KTP) Single Crystal. *J. Phys. Soc. Jpn.* **1993**, *62*, 183–195.

(27) Park, J.-H.; Choi, B.-C., Kim, J.-B. Electrical Properties of $KTiOPO_4$ Single Crystal in the Temperature Range from –100°C to 100°C. *Solid State Comm.* **2004**, *130*, 533–536.

SYNOPSIS TOC (Word Style “SN_Synopsis_TOC”).

Insert Table of Contents artwork here